

## Supporting Information

### **Cross-scale honeycomb architecture-based flexible piezoresistive sensor for multiscale pressure perception and fine-grained identification**

Chenxi Lu<sup>1,3</sup>, Yuan Gao<sup>1</sup>, Xiaobao Chan<sup>1</sup>, Wei Yu<sup>2</sup>, Haifeng Wang<sup>2</sup>, Liang Hu<sup>1,3</sup> & Lingwei Li<sup>1,2\*</sup>

<sup>1</sup> *Key Laboratory of Novel Materials for Sensor of Zhejiang Province, College of Materials and Environmental Engineering, Hangzhou Dianzi University, Hangzhou 310012, P.R. China*

<sup>2</sup> *Key Laboratory of Electromagnetic Processing of Materials (Ministry of Education), School of Materials Science and Engineering, Northeastern University, Shenyang 110819, P.R. China*

<sup>3</sup> *State Key Laboratory of Silicon and Advanced Semiconductor Materials, Zhejiang University, Hangzhou 310027, P.R. China*

\* Email: Lingwei Li (lingwei@hdu.edu.cn)

## Figures and captions

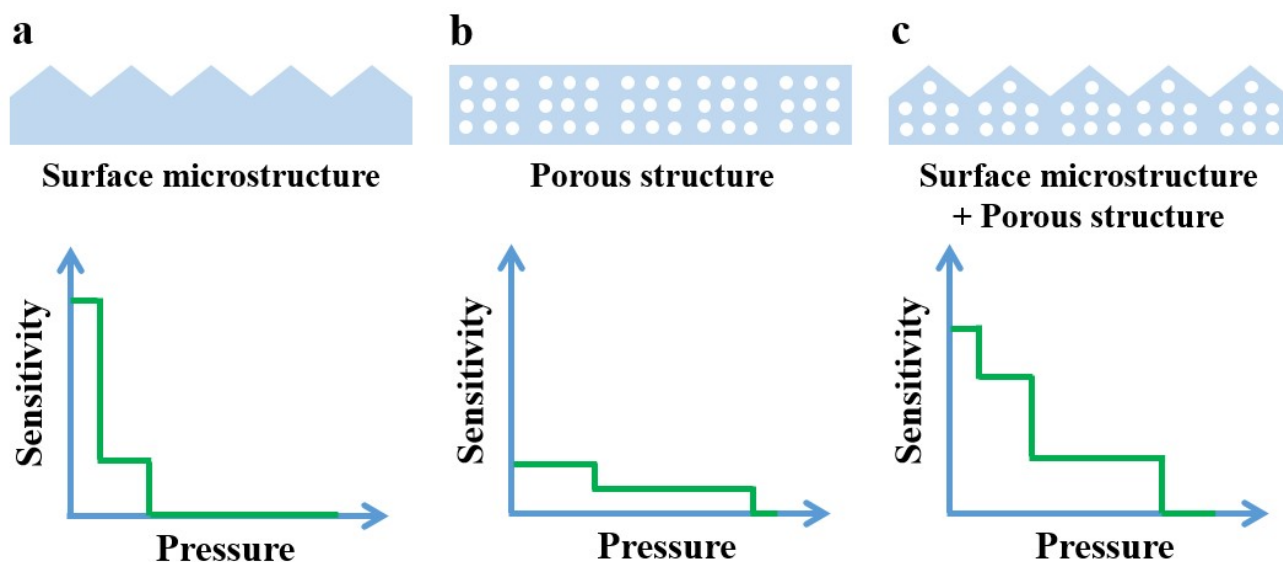


**Figure S1.** Relationship of sensitivity with pressure for the piezoresistive pressure sensors based on various structures. a) Surface microstructure. b) Porous structure. c) Combination of surface microstructure and porous structure.

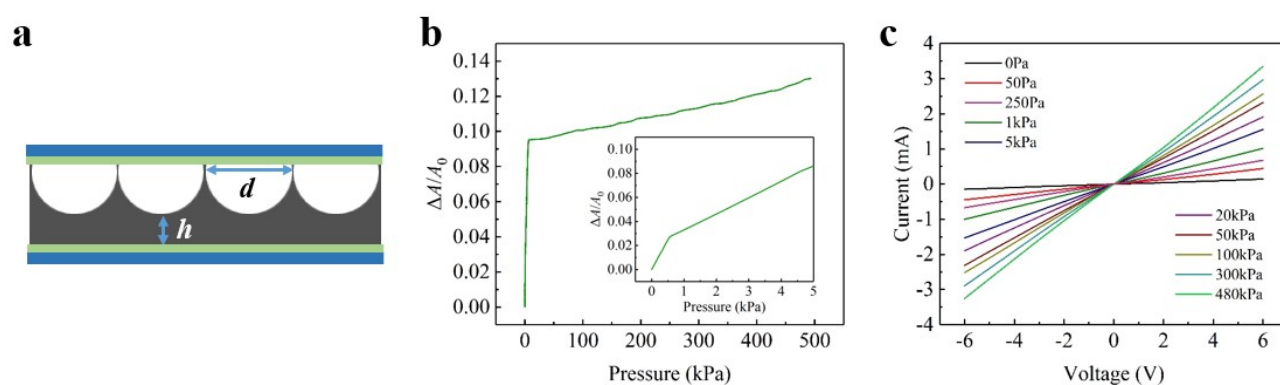


**Figure S2.** a) Scheme illustration of lateral view of the CHA-based piezoresistive pressure sensor. b) The increase in the contact area  $A$  between the up electrode and the CHA3-P sensor layer with pressure according to the FEA, in which  $A_0$  is the original contact area. c) The current-voltage characteristics of the CHA3-P sensor at no applied pressure and also at different applied pressures.

**Table S1.** The structure parameters of the honeycomb diameter  $d$  and base layer thickness  $h$  of the sensors.

	$d$ (mm)	$h$ (um)
Plane	0	750
CHA2	2.00	0
CHA2-P	2.00	750
CHA3-P	3.00	750
CHA4-P	4.00	750

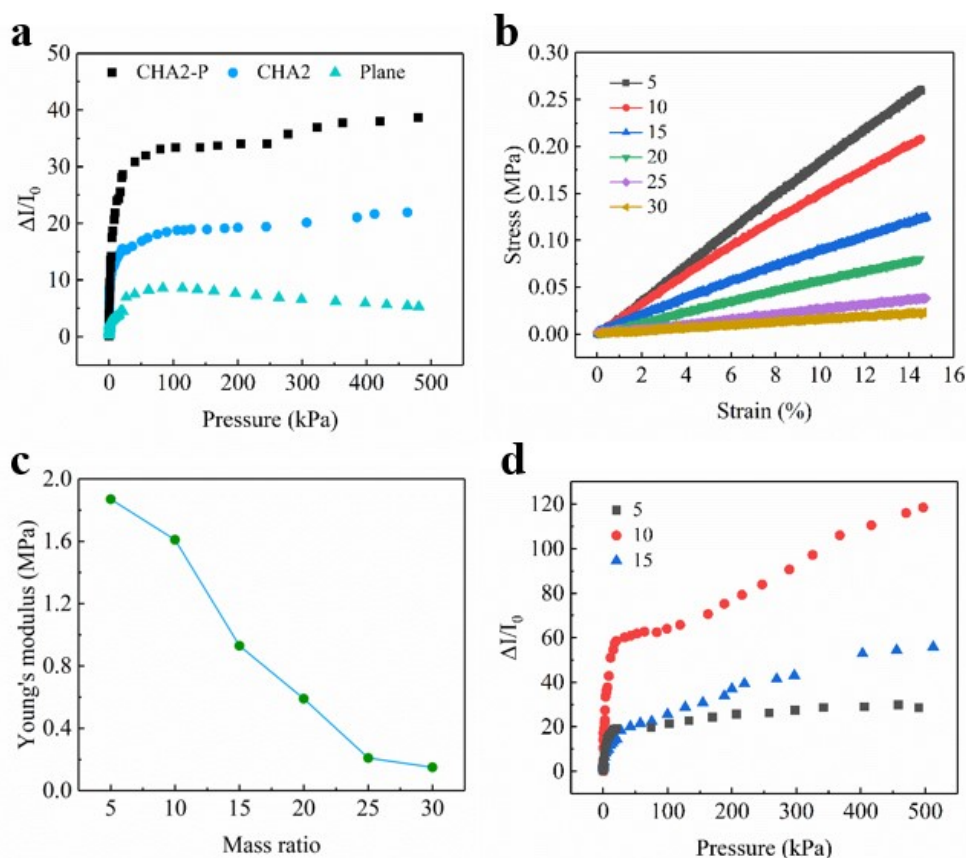


**Figure S3.** Comparison of the sensing performances of the sensors based on various structures and Young's modulus. a) Relative current changes of the sensors based on different structures over a broad pressure regime up to 460 kPa. b) Stress-strain curves of the PDMS with different mass ratios of pre-polymer and cross-linker. c) Relationship of Young's modulus with the mass ratio. d) Relative current changes of the CHA-based sensors with different Young's modulus over a broad pressure regime up to 460 kPa.

**Table S2.** The sensitivity for the CHA2-P, CHA3-P, and CHA4-P sensors for the three pressure regimes.

CHA2-P	Pressure (kPa)	0.0005 – 0.11	0.11 – 21.17	21.17 – 460
	Sensitivity (kPa <sup>-1</sup> )	32.41	1.16	0.02
CHA3-P	Pressure (kPa)	0.0005 – 0.56	0.56 – 20.40	20.40 – 460
	Sensitivity (kPa <sup>-1</sup> )	27.97	2.30	0.13
CHA4-P	Pressure (kPa)	0.0005 – 0.11	0.11 – 20.30	20.30 – 460
	Sensitivity (kPa <sup>-1</sup> )	14.41	0.38	0.01

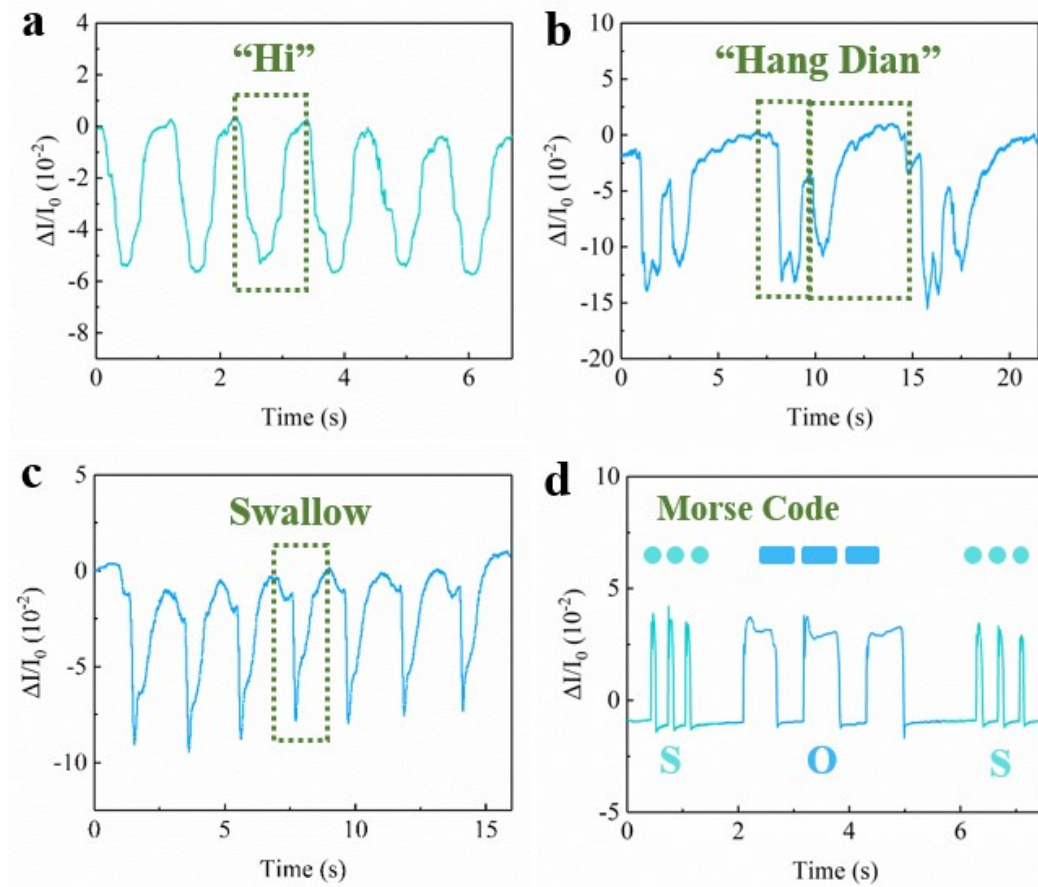


**Figure S4.** Pressure perception and fine-grained identification in low-pressure regime. Relative current changes during the pronunciations of a) “Hi” and b) “Hang Dian”. c) Relative current changes during swallow. d) Morse code “SOS” encoded by controlling the action time and interval of the weak airflow or tapping.

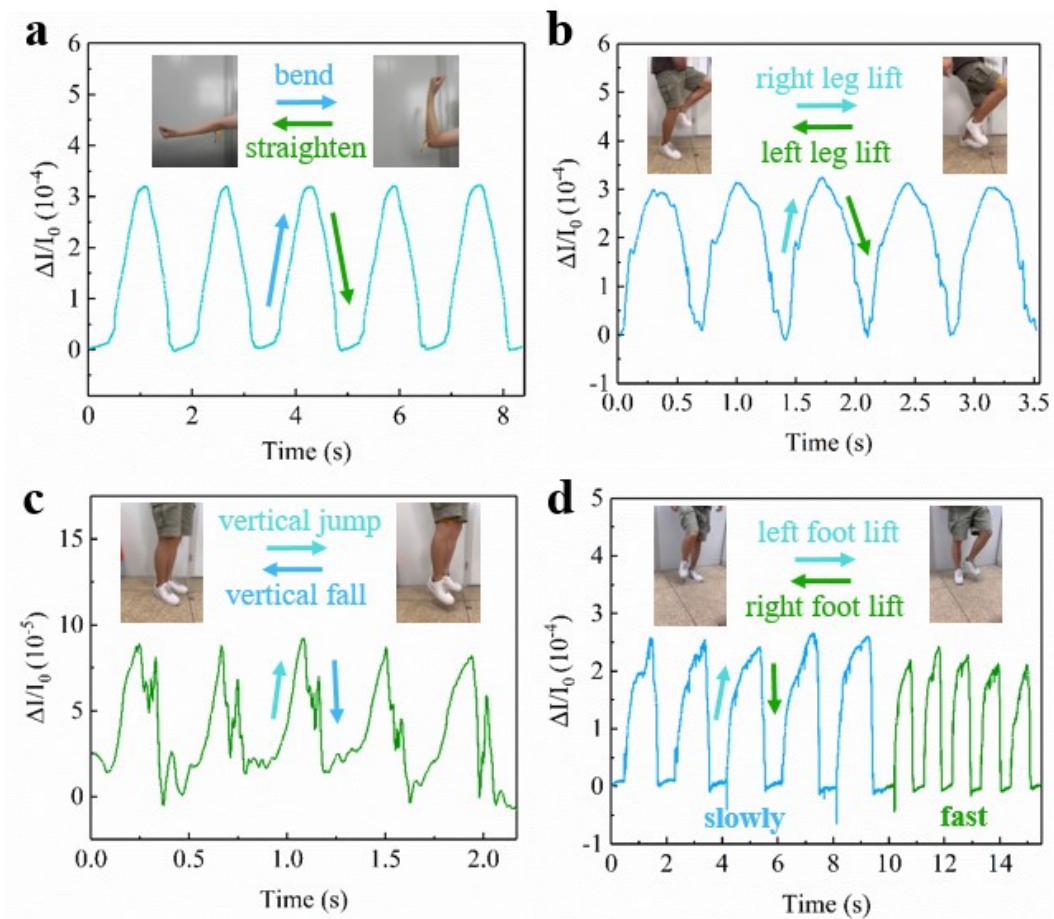


**Figure S5.** Motion monitoring and identification. Relative current changes of different motions including a) elbow bending/straightening, b) leg lifting alternately, c) vertical jump/fall, and d) foot lifting alternately.